36th International Electric Vehicle Symposium and Exhibition (EVS36)
Sacramento, California, June 11-14, 2023

A Novel Approach for a Predictive Online ECMS Applied in Electrified Vehicles Using Real Driving Data

Felix Deufel*, Malte Freund, Frank Gauterin
**Correspondence: felix.deufel@kit.edu*
Institute of Vehicle Systems Technology, Karlsruhe Institute of Technology, 76131 Karlsruhe, Germany

Executive Summary

To increase the efficiency of electrified vehicles, many energy management strategies (driving strategies) have been proposed. These include both offline optimization techniques to identify a system's theoretical optimum and online optimization techniques created for onboard use in the vehicle. In this study, a new approach for a predictive online strategy is presented, which is investigated on a D-segment vehicle powered by a 48 V hybrid electric system in a P2 topology. It is demonstrated how this so-called predictive Online Equivalent Consumption Minimization Strategy (ECMS) can achieve additional fuel savings compared to a non-predictive Online ECMS by using map data. The investigations are limited to the consideration of traffic signal (TS) positions on the upcoming route. Simulation results focus on the interaction between the energy management strategy (EMS) and usable battery energy.

1 Introduction

Due to emission regulations and an increase in environmental consciousness in general, a broad variety of alternative drive systems have been developed. These include 48 V hybrid electric vehicles (HEVs), which have the benefit of greatly decreasing CO2 emissions at moderate system expense, especially for inner-city driving. A 48 V system is described by component dimensioning, topology, and an energy management strategy (EMS) [1]. The EMS has to guarantee a robust operation in various driving situations. An overview of the most common methods provided within [1–8] shows that EMS development had been extensively researched over last years. In this paper, a novel approach for a predictive Online ECMS is presented using real driving cycles. It is demonstrated how, in the case of a known journey and the availability of map data, a predictive Online ECMS is established by using the present Global Navigation Satellite System (GNSS) position. This is the case, for instance, when manually entering a route into a navigation system or returning to a previously travelled path which is identified by intelligent algorithms. It is shown, how a predictive Online ECMS can achieve additional fuel savings compared to a non-predictive Online ECMS by predicting recuperation events due to traffic signals (TS). The simulation results focus on the interaction between the EMS and battery.

2 Related Work

EMS can be subdivided in multiple ways. They can be categorized into rule-based, optimization-based, and learning-based techniques. Mixed forms also exist. Furthermore, offline and online methods can be distinguished. *Offline strategies* are defined by the need for prior knowledge of the whole driving profile. With this, a specific hybrid design is described for instance in terms of possible fuel consumption savings for a certain cycle. The global optimum is determined for benchmark analysis. *Online strategies* require only limited prior knowledge of the upcoming driving path. The ECMS which is investigated in this work can be assigned to optimization-based EMS concepts. Depending on the particular implementation, an ECMS is associated with either the offline or online techniques. Using an Offline ECMS, the global optimum for time-invariant systems is found due to the equivalence to Pontryagin's minimum principle (PMP) [10, 11], where a so-called equivalence factor λ is found iteratively to solve the optimization problem [12, 13]. This Offline ECMS is frequently utilized to find the global optimum in offline applications, especially due to the low computing effort [14]. The 2D-ECMS has been created to investigate topologies with two traction motors [15]. For an Online ECMS, which was first published by Paganelli et al. [16], the idea of an SOC-dependent control of the equivalence factor λ was effectively implemented [9,17–26]. In addition, there are predictive Online ECMS techniques where predictions are essential for the ECMS's fundamental operation [19, 31]. However, it has also been demonstrated that the introduction of predictive information can enhance a non-predictive Online ECMS implementation. The following publications should be mentioned:

- In [36], step functions are used for adjusting λ by taking into account the future energy demand. A 10% improvement compared to a non-predictive Online ECMS solution was reached.
- In [35], optimal recuperation is realized by predictive charging and discharging of the battery. A 6 % improvement compared to a non-predictive Online ECMS solution is achieved.
- In [38], velocity prediction using a Convolutional Neural Network (CNN) for optimal λ determination is realized. A 0.2 % to 0.5 % improvement compared to the non-predictive Online ECMS is presented.
- In [34], velocity prediction is used to determine *SOC nodes*. A 9.7 % improvement compared to the non-predictive Online ECMS solution is given.
- In [37], λ adaptation is realized considering future energy demand with a dynamic prediction horizon. An improvement between 0.3 % and 4 % compared to the non-predictive Online ECMS is achieved.
- In [33], velocity prediction at intersections considering traffic signal (TS) state and traffic flow leads to an improvement of 0-2 % compared to the non-predictive Online ECMS.

The presented prediction approaches show a wide range of possibilities for the development of predictive driving strategies. When comparing the results, it should be noted that different boundary conditions, vehicle models, and types of ECMS were used in each publication. The approach of [36], for example, has only been tested on previously known very hilly routes and is therefore only useful in very specific scenarios. Therefore, a comparison and evaluation of the results is of limited value. However, for the authors of the paper, these investigations form the basis for developing an own predictive approach. In [29], an own approach utilizing the recuperation potential has already been published. It was shown that noticeable CO2 reduction potentials occur in particular with limited battery capacity. Detailed investigations regarding predicting torque for predictive EMS are presented in [28] and [30]. However, it was shown that the prediction of the future torque is very difficult and often only possible with a certain degree of uncertainty. Therefore, this paper presents a novel approach for a predictive Online ECMS considering recuperation potentials using map data without the need for torque predictions. Additionally, a comparison to an Online ECMS that is not predictive is provided.

3 Modelling

In vehicle simulation, forward and backward simulation can be distinguished. Forward simulation models are based on the physical causality of the system by comparing the target velocity with the actual vehicle velocity using a driver model. A velocity can then be calculated for each time step based on the acceleration brought on by the control input of the driver model. In contrast, a backward simulation model, presupposes that the vehicle adheres to a predetermined profile of acceleration and velocity. Therefore, no driver model is necessary [4]. The verified backward calculation model of a 48 V HEV (P2 topology, see Figure 1) with an Offline ECMS and an iteratively calculated λ from the work of [14] is used in this work.

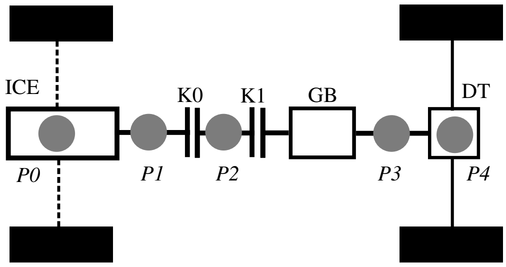

Figure 1: Topologies of HEVs in parallel configuration from [29].

In this model torque is calculated from the longitudinal dynamics of the vehicle. Hereby, the wheel radius as well as the transmission ratios of the vehicle are taken into account. The correlations from longitudinal dynamics are shown below. The different parameters and their corresponding units are listed in Table 1.

$$F_{Wheel} = F_{air} + F_{roll} + F_{acc} + F_{slp} \tag{1}$$
$$F_{air} = c_w \cdot A \cdot \frac{\rho}{2} \cdot v^2 \tag{2}$$
$$F_{roll} = m \cdot g \cdot cos\alpha \cdot f_R \tag{3}$$
$$F_{acc} = m \cdot a \tag{4}$$
$$F_{slp} = m \cdot g \cdot sin\alpha \tag{5}$$

Table 1: Parameters and units of the driving resistances.

Drag Coefficient	c_w	0.3
Projected Frontal Area	A	2.5 m^2
Air Density	ρ	1.2 kg/m^3
Vehicle Mass	m	1600 kg
Gravitational Acceleration	g	9.81 m/s^2
Rolling Resistance Coefficient	f_R	0.012

Internal combustion engine (ICE), electric motor (EM), and gearbox (GB) are modelled using stationary maps. The 48 V battery is represented by a simple inner resistance model. Equations 6 and 7 are used to compute the battery voltage under load U_{bat} and the corresponding battery current I_{bat}. Therefore, the battery power P_{em}, the battery losses $P_{em,loss}$, and the power from auxiliary consumers P_{aux} are considered. Moreover, the open-circuit voltage U_{OCV} and the inner resistance R_i are required. In addition, as a measure of energy deviation from the starting conditions, an energy deviation dE from reference SOC is calculated (Equation 8). It is used as a criterion for a neutral energy balance. [29]

$$I_{bat} = \frac{P_{em} + P_{em,loss} + P_{aux}}{U_{bat}} \tag{6}$$

$$U_{bat} = U_{OCV}(SOC) - R_i(SOC) \cdot I_{bat} \tag{7}$$

$$dE = \int U_{bat} I_{bat} dt \tag{8}$$

The battery is of a nickel–mangan–cobalt/graphite cell type. R_i and U_{OCV} are calculated using SOC-specific component data. However, for simplification a large 48V battery ($>$10 kWh) with constant SOC characteristics (SOC = 70%) is used within the investigations. Other effects, such as degradation of the battery and its impact on CO_2 emissions, are neglected [14]. The recuperated energy is determined using a simplified logic considering the limits of the electrical components and the application of the mechanical brake.

The studies are based on real driving cycles including four different drivers. These real driving cycles were already used and presented in [28] and [30]. Hereby, relevant map data from Open Street Map (OSM) was matched with the original GNSS tracks according to Figure 2 and Figure 3. For detailed information on the preprocessing of the driving data, please refer to [30].

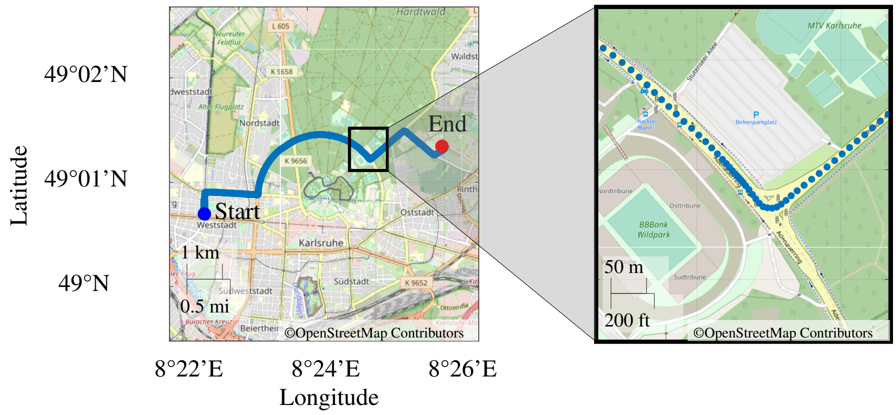

Figure 2: Visualization of available driving data. From [30].

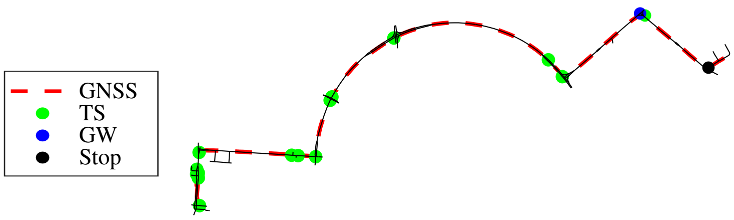

Figure 3: Visualisation of identified Open Street Map (OSM) Data including GNSS track, traffic signal (TS), give way (GW), and stop. From [30].

This publication is limited to the cycles of *Driver 1*, which covers 63 cycles of city driving, country road driving, and highway driving of a total duration of 30 h and almost 3000 km (for more information see [28]). For the design of a non-predictive Online ECMS, three representative cycles are selected for each road type. These nine cycles should represent real operation as good as possible. The most important characteristics are shown below (Table 2).

Table 2: Real driving cycles to parametrize non-predictive Online ECMS.

Road Type	Avg. velocity in km/h	Max. velocity in km/h	Distance in km	Duration in h	Stand-still in %
City	28	69	6	0.2	26
	19	60	4	0.2	39
	25	62	11	0.4	21
Country Road	73	110	39	0.5	1
	57	90	17	0.3	6
	67	118	41	0.6	5
Highway	108	168	164	1.5	2
	116	189	162	1.4	1
	101	176	74	0.7	6

In Figure 4, the traffic signal (TS) density is shown for each cycle. Cycles marked in dark gray are selected for the exemplary application of the newly developed predictive Online ECMS approach. The chosen cycles are characterized by at least one TS per km.

4 Methodology

In the concept of an ECMS, an equivalent fuel consumption is calculated taking into account the fuel's lower heating value, Q_{lhv}, and an equivalence factor λ to convert battery power into fuel power. Using the equivalent fuel consumption, a cost function J is stated, where the optimization problem P is written as follows [14]:

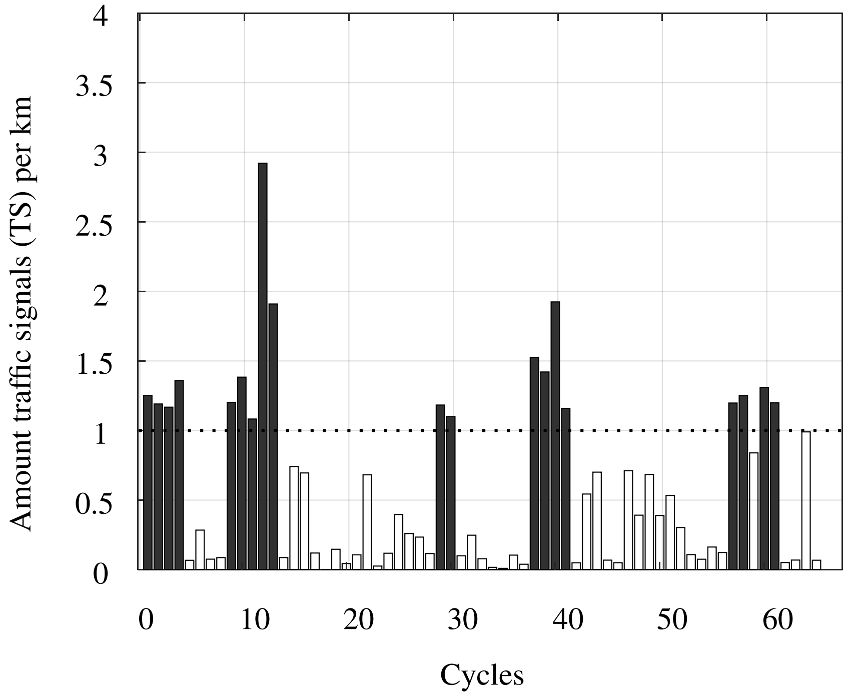

Figure 4: Overview of the 63 driving cycles. As the investigations are limited to the consideration of TS positions, TS per km are shown for each cycle. Cycles marked in dark gray are selected for the exemplary application of the newly developed predictive Online ECMS approach. These cycles are characterized by at least one TS per km.

$$P : \min_{u} \int J(u,x)dt \tag{9}$$

$$J(u,x) = \dot{m}_{fuel} + \lambda \frac{P_{bat}}{Q_{lhv}} \tag{10}$$

At each time step, the ideal torque split is determined by minimizing P. In an Offline ECMS a constant λ is found iteratively for time-invariant systems. For an online-capable implementation of the ECMS, the idea of an SOC-dependent control of the equivalence factor λ was implemented in several studies [9, 17–26]. In this work, an average equivalence factor $\lambda_{Offline,avg}$ is used for the Online ECMS. However, this does not guarantee charge-sustaining (CS) behavior in online operations: Depending on the cycle, the SOC trajectories result in an excessive charging or discharging of the battery. Therefore, a penalty term is added. According to $dSOC$ (difference between the real SOC and the reference SOC), the value of the energy (λ) is either raised or lowered. As concluded in [26, 32], the trigonometric penalty function is better than a proportional penalty function: It allows tiny deviations from the reference SOC, but strongly penalizes significant deviations. Therefore, the penalty term consists of the penalty factor kp_{SOC} multiplied by the cubic derivation of SOC $dSOC^3$ (see Equation 11). In terms of CS operation, the deviation of the battery's energy content at the end of the cycle is limited to a specific value. These presumptions are used to establish the proper kp_{SOC} for the non-predictive Online ECMS.

$$\lambda(t) = \lambda_{Offline,avg} - kp_{SOC} \cdot dSOC(t)^3 \tag{11}$$

In this paper, a novel approach for a predictive Online ECMS which considers map data to achieve savings potentials compared to the non-predictive Online ECMS implementation is presented. The investigations are limited to the consideration of TS positions on the upcoming route. The appearance of a TS within the upcoming horizon (represented by $flag_{TS}$) has a direct impact on λ using an additional parameter kp_{TS}:

$$\lambda(t) = \lambda_{Offline,avg} - kp_{SOC} \cdot dSOC(t)^3 - kp_{TS} \cdot flag_{TS} \tag{12}$$

A summary of the applied methodology is given by Figure 5.

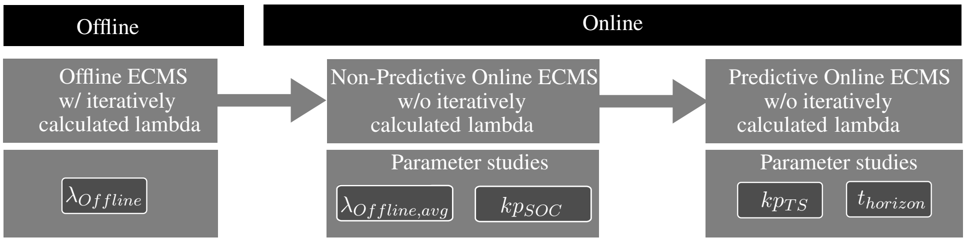

Figure 5: Applied methodology for predictive Online ECMS.

5 Results

First, the Offline ECMS is used to iteratively determine the optimum $\lambda_{Offline}$ value for each of the nine cycles selected (Table 2). An overview is given in Table 3. $\lambda_{Offline}$ ranges from 2.55 to 2.88.

Table 3: Results from Offline ECMS for real driving cycles from Table 2.

Road Type	λ_{Offline}	**CO2 (g/km)**
City	2.61	134.16
	2.55	139.87
	2.61	144.42
Country Road	2.74	124.69
	2.70	122.31
	2.64	172.21
Highway	2.81	148.40
	2.75	168.92
	2.88	169.08

The non-predictive Online ECMS is parametrized according to [29]. In contrast to [29], the journey itself and the Global Navigation Satellite System (GNSS) position are assumed to be known for this predictive Online ECMS. It is also expected that the appropriate map data is available. Cycles with high TS density are typically city driving cycles. Therefore, the parametrization of the non-predictive Online ECMS focuses on city driving cycles. A $\lambda_{Offline,avg,city}$ of 2.60 is chosen (Table 4). Parameter studies, which will not be discussed in detail here, result in a kp_{SOC} of 3.57 to achieve charge-sustaining (CS) operation. For further information the reader is referred to [29]. A battery-specific parametrization of the non-predictive Online ECMS is waived in this publication.

Table 4: Final parametrization for non-predictive Online ECMS.

$\lambda_{Offline,avg,city}$	2.60
kp_{SOC}	3.57

In the next step, a predictive Online ECMS is to be parametrized to show additional savings potentials for known routes with a high density of TS (Figure 4). Therefore, both parameters kp_{TS} and horizon length $t_{horizon}$ have to be specified. The investigations will be carried out for different battery sizes. Parameter ranges to identify the best parametrization of kp_{TS} and $t_{horizon}$ are given in Table 5.

Table 5: Ranges to identify optimal parameters kp_{TS} and horizon length $t_{horizon}$ of the predictive Online ECMS for a usable battery energy of *25 Wh, 50 Wh, 75 Wh, 100 Wh, 200 Wh, 300 Wh, 400 Wh, 500 Wh*, and *1000 Wh*.

	min	max
kp_{TS}	0	5
$t_{horizon}$ in s	5 s	100 s

In Figure 6, CO2 reduction potentials in % over kp_{TS} for different $t_{horizon}$ in the case of a usable battery energy of 25 Wh are given for the selected cycles with high TS density from Figure 4. For formatting reasons, the plots are restricted to 16 out of 19 cycles. It is concluded that above a certain value of kp_{TS}, there is no further influence on CO2. For each cycle, there exists an individual kp_{TS} with a corresponding $t_{horizon}$ which leads to the best results. However, to ensure robust applicability, a parametrization for the overall largest CO2 savings potential for each battery size can be determined based on these investigations.

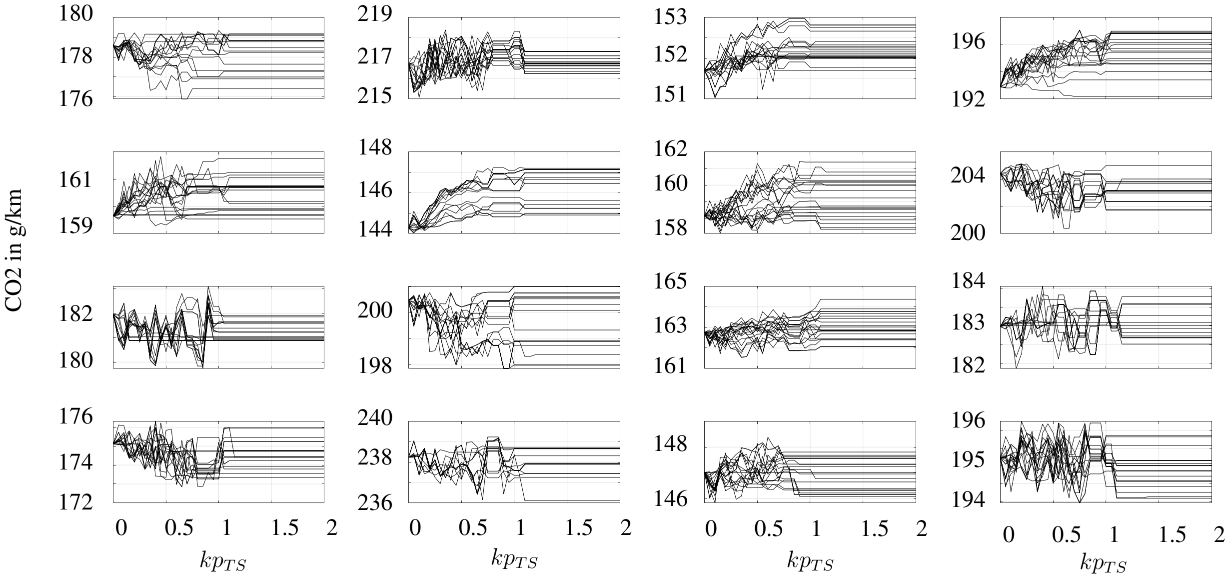

Figure 6: Usable battery energy 25 Wh: CO2 over kp_{TS} of several $t_{horizon}$ for predictive Online ECMS (16/19 cycles). Each graph represents a specific $t_{horizon}$.

A behavior similar to that shown in Figure 6 is seen for a usable battery energy of 100 Wh in Figure 7.

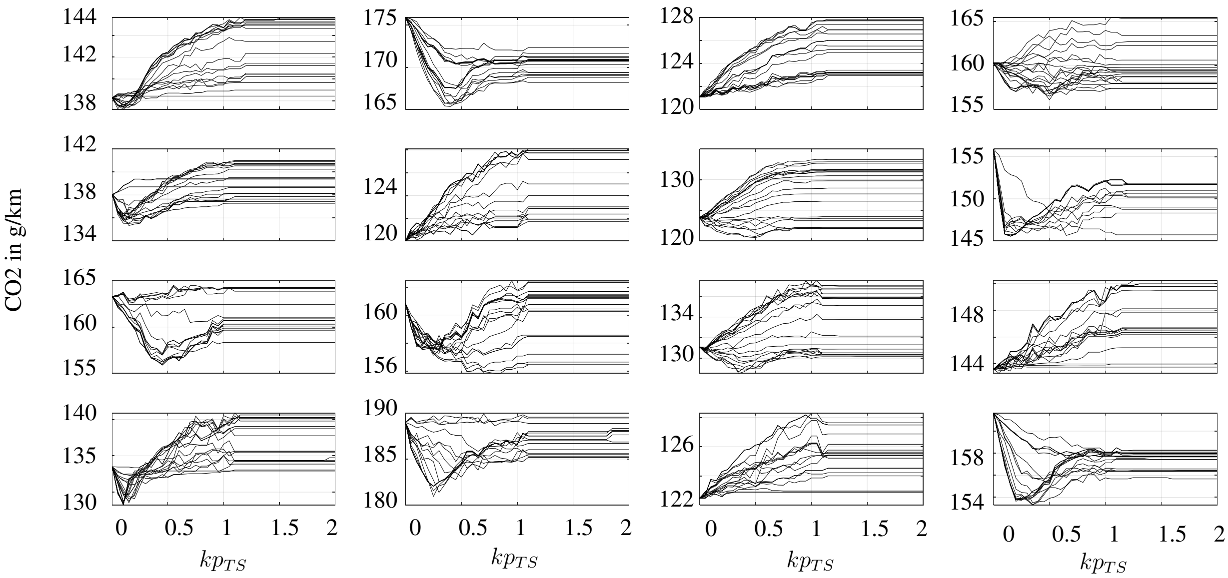

Figure 7: Usable battery energy 100 Wh: CO2 over kp_{TS} of several $t_{horizon}$ for predictive Online ECMS (16/19 cycles). Each graph represents a specific $t_{horizon}$.

In Figure 8, the velocity, the presence of a TS, and the SOC trajectories are presented over time for an exemplary cycle (100 Wh usable battery energy). This includes both the non-predictive Online ECMS and the predictive Online ECMS for the chosen $\lambda_{Offline,avg,city}$ = 2.60 using the ideal kp_{TS} and $t_{horizon}$ setting for a usable battery energy of 100 Wh. Additionally, the SOC trajectory is given for a non-predictive Online ECMS with a λ of 2.70.

In a first step, analysis focuses on both the non-predictive and the predictive Online ECMS for $\lambda_{Offline,avg,city}$ = 2.6. At t = 380 s, more recuperation potential is used, when λ is reduced by applying the predictive

Online ECMS. At t = 200 s, by contrast, fuel consumption increases, as SOC_{min} is kept for a longer time, which typically leads to additional operation of the ICE. At t = 300 s, there are no major effects on the optimality of the EMS.

The strict reduction of λ whenever a TS is encountered can locally degrade the optimality of the predictive Online ECMS. The degree of degradation depends on how many TS actually do not affect the velocity. At t = 500 s, for example, only minor influence of the existing TS on the velocity profile can be detected. Apart from that, if the stationary phase is long enough, energy consumption by the auxiliary consumers might overcompensate the recuperated energy so that no reduction of λ is needed. In these investigations, however, auxiliary consumers are significantly lower compared to the rise by recuperated energy (t = 400 s). Overall a well parametrized predictive Online ECMS leads to a reduction in fuel consumption compared to the non-predictive Online ECMS.

In a second step, the SOC trajectory for λ of 2.70 should also be considered. A closer look at the non-predictive SOC trajectorys of $\lambda_{Offline,avg,city}$ = 2.60 and λ of 2.70 reveals that CO2 reduction potentials by applying a predictive Online ECMS are highly dependent on the chosen non-predictive basic implementation: At t = 380 s, the additional energy hub for the use of recuperated energy is much higher for λ of 2.70 than for $\lambda_{Offline,avg,city}$ = 2.60. Anyway, both non-predictive Online ECMS implementations reach the upper SOC limit multiple times and therefore both λ seem to be too high for the specific driving cycle. It is concluded that significant savings potentials can already be achieved by an adequate choice of non-predictive Online ECMS. At the same time, however, the additional savings from the proposed predictive Online ECMS using recuperation potentials compared to a non-predictive implementation are reduced.

As already stated before, Figure 8 reveals that λ reductions also occur when the battery is already discharged before a recuperation phase is initiated (t = 200 s). Therefore, a dependence of kp_{TS} on SOC is introduced in a follow-up work. Thus, when SOC is around the lower limit, no reduction of the value of the electric energy (λ) is allowed. Apart from this measure, also a dependence of kp_{TS} on the occurrence of the recuperation potential in the prediction horizon could be added. If the TS is quite close, the influence should be large. If the TS is in the later part of the studied horizon, the influence is reduced.

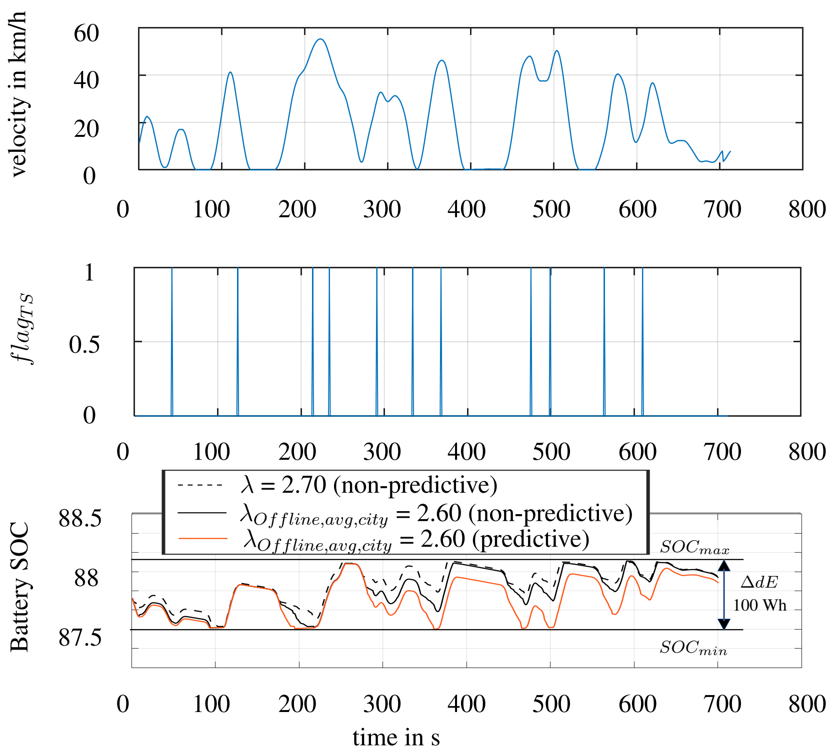

Figure 8: Usable battery energy 100 Wh: Velocity (upper graph), $flag_{TS}$ (middle graph), and battery SOC over time (lower graph). Both for non-predictive Online ECMS (blue) and predictive Online ECMS (orange) with $t_{horizon}$: 65 s, kp_{TS} = 0.2. In addition, the course for the non-predictive Online ECMS with λ = 2.70 is plotted.

In contrast to Figure 6 and Figure 7, there are no additional savings potentials for a predictive implementation when a large battery (usable battery energy 1000 Wh) is used, see Figure 9. Here, a significant deterioration is observed for all kp_{TS}. This is in line with the findings already made in the context of [29] that the considering recuperation potentials in a predictive Online ECMS does not lead to any noticeable savings potential for large batteries compared to a well parametrized non-predictive Online ECMS.

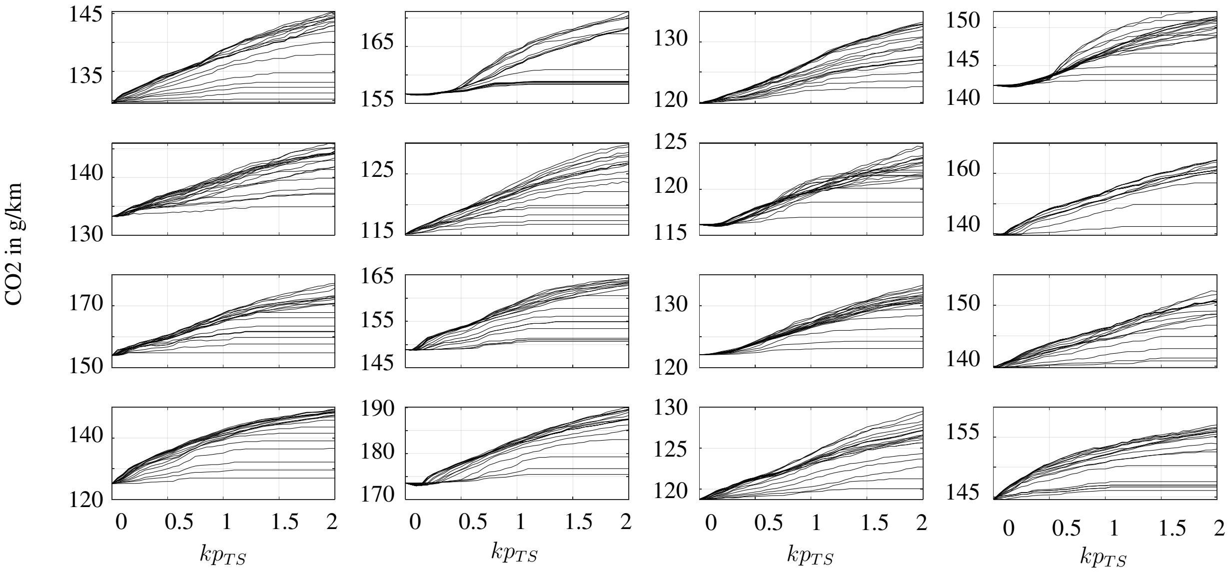

Figure 9: Usable battery energy 1000 Wh: CO2 over kp_{TS} of several $t_{horizon}$ for predictive Online ECMS (16/19 cycles). Each graph represents a specific $t_{horizon}$.

As can be seen in Figure 10, an overall improvement is observed when applying a predictive Online ECMS. However, the savings potentials depend strongly on the usable energy content of the battery. The highest savings potentials exist with a usable battery energy of 100 Wh. With lower battery capacities, the savings potentials using a predictive implementation become less. For a usable battery energy larger than 100 Wh, no more significant savings potentials are found. The corresponding parameters for each battery size are listed in Table 6.

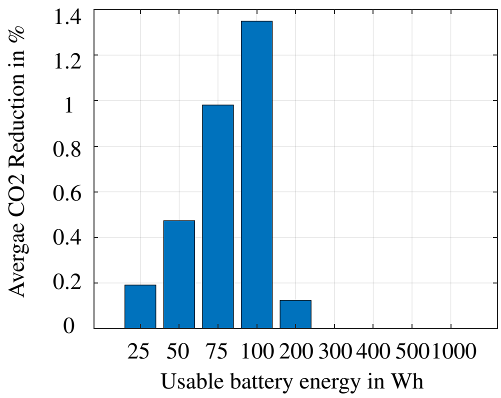

Figure 10: Potentials of the proposed predictive EMS for different usable battery energies: Average CO2 reduction in % when applying the predictive Online ECMS compared to the non-predictive Online ECMS.

Table 6: Optimal overall parameters of the predictive Online ECMS for different battery sizes including average CO2 reduction potentials compared to the non-predictive Online ECMS (Figure 10).

Usable energy in Wh	$\mathbf{kp_{TS}}$	**Horizon in s**	**Reduction CO2 %**
25	0.35	30	0.19
50	0.15	40	0.47
75	0.35	45	0.98
100	0.20	50	1.35
200	0.05	25	0.12
300			
400	*No additional CO2 reduction potentials by applying*		
500	*the proposed predictive Online ECMS considering TS*		
1000			

6 Conclusions

It is demonstrated that a predictive Online ECMS can achieve additional fuel savings compared to a non-predictive Online ECMS by using map data. Within this investigations TS from the upcoming road profile are considered in the predictive Online ECMS, whereby more than 1 % average savings potentials compared to a non-predictive implementation were shown. The highest savings potentials are found with a usable battery energy of 100 Wh. With lower usable battery energy, the savings potentials decrease using the proposed predictive implementation. For batteries larger than 100 Wh, no more significant savings potentials are found. Furthermore, a big dependence of the added value by implementing a predictive Online ECMS from the basic non-predictive Online ECMS is revealed.

For further investigations the methodology will be applied to a bigger dataset. As already stated a dependence of kp_{TS} on SOC and the occurrence of the recuperation potential in the prediction horizon will be added. Apart from that, the predictive Online ECMS will be enhanced by using additional map data, telemetry data or information from Radar, Lidar, and camera. Also Car-to-Car (C2C) and Car-to-X (C2X) communication could be used to consider the status of the traffic signal. For an implementation in a real vehicle, the upcoming velocity has to be approximated to transfer map information from the distance domain to the time domain. Alternatively, a specific future distance could be used instead of the specified time horizon.

Acknowledgments

The authors would like to thank Mercedes-Benz AG for funding this project.

References

[1] Silvas, E.; Hofman, T.; Murgovski, N.; Etman, P.; Steinbuch, M. Review of Optimization Strategies for System-Level Design in Hybrid Electric Vehicles. *IEEE Transactions on Vehicular Technology* **2016**, p. 1.

[2] Tran, D.D.; Vafaeipour, M.; El Baghdadi, M.; Barrero, R.; van Mierlo, J.; Hegazy, O. Thorough state-of-the-art analysis of electric and hybrid vehicle powertrains: Topologies and integrated energy management strategies. *Renewable and Sustainable Energy Reviews* **2020**, *119*, 109596.

[3] Serrao, L. A Comparative Analysis Of Energy Management Strategies For Hybrid Electric Vehicles. PhD thesis, 2009.

[4] Onori, S.; Serrao, L.; Rizzoni, G. *Hybrid Electric Vehicles*; Springer London: London, 2016.

[5] Rizzoni, G.; Onori, S. Energy Management of Hybrid Electric Vehicles: 15 years of development at the Ohio State University. *Oil & Gas Science and Technology – Revue d'IFP Energies nouvelles* **2015**, *70*, 41–54.

[6] Salmasi, F.R. Control Strategies for Hybrid Electric Vehicles: Evolution, Classification, Comparison, and Future Trends. *IEEE Transactions on Vehicular Technology* **2007**, *56*, 2393–2404.

[7] Xu, N.; Kong, Y.; Chu, L.; Ju, H.; Yang, Z.; Xu, Z.; Xu, Z. Towards a Smarter Energy Management System for Hybrid Vehicles: A Comprehensive Review of Control Strategies. *Applied Sciences* **2019**, *9*, 2026.

[8] Jiang, Q.; Ossart, F.; Marchand, C. Comparative Study of Real-Time HEV Energy Management Strategies. *IEEE Transactions on Vehicular Technology* **2017**, *66*, 10875–10888.

[9] A. Chasse.; A. Sciarretta.; J. Chauvin. Online optimal control of a parallel hybrid with costate adaptation rule **2010**.

[10] Kim, N.; Cha, S.; Peng, H. Optimal Control of Hybrid Electric Vehicles Based on Pontryagin's Minimum Principle. *IEEE Transactions on Control Systems Technology* **2011**, *19*, 1279–1287.

[11] Kim, N.; Rousseau, A. Sufficient conditions of optimal control based on Pontryagin's minimum principle for use in hybrid electric vehicles. *Proceedings of the Institution of Mechanical Engineers, Part D: Journal of Automobile Engineering* **2012**, *226*, 1160–1170.

[12] Serrao, L.; Onori, S.; Rizzoni, G. ECMS as a realization of Pontryagin's minimum principle for HEV control. 2009 American Control Conference. IEEE, 2009, pp. 3964–3969.

[13] Zheng, C.H. Numerical Comparison Of Ecms And Pmp-Based Optimal Control Strategy In Hybrid Vehicles. International Journal of Automotive Technology, Vol. 15, No. 7, pp. 1189-1196 (2014)

[14] Foerster, D.; Decker, L.; Doppelbauer, M.; Gauterin, F. Analysis of CO2 reduction potentials and component load collectives of 48 V-hybrids under real-driving conditions. *Automotive and Engine Technology* **2021**, *6*, 45–62.

[15] Mayer, A. Two-Dimensional ECMS for System Analysis of Hybrid Concepts featuring Two Electric Traction Motors. In Proceedings of the 2019 International Symposium on Systems Engineering (ISSE), Edinburgh, UK, 1–3 October 2019

[16] Paganelli, G.; Delprat, S.; Guerra, T.M.; Rimaux, J.; Santin, J.J. Equivalent consumption minimization strategy for parallel hybrid powertrains. Vehicular Technology Conference. IEEE 55th Vehicular Technology Conference. VTC Spring 2002 (Cat. No.02CH37367). IEEE, 6-9 May 2002, pp. 2076–2081.

[17] Onori, S.; Serrao, L. On Adaptive-ECMS strategies for hybrid electric vehicles. Les Rencontres Scientifiques d'IFP Energies nouvelles – Int. Scient. Conf. on hybrid and electric vehicles – RHEVE 2011 6-7 December 2011

[18] Simona Onori, Lorenzo Serrao, Giorgio Rizzoni. Adaptive Equivalent Consumption Minimization Strategy for Hybrid Electric Vehicles **2010**.

[19] Cristian Musardo.; Giorgio Rizzoni.; Benedetto Staccia. *A-ECMS: An Adaptive Algorithm for Hybrid Electric Vehicle Energy Managemen: Proceedings, December 12 - 15, 2005, Seville, Spain*; IEEE Operations Center: Piscataway, NJ, 2005.

[20] Kessels, J.; Koot, M.; van den Bosch, P.; Kok, D.B. Online Energy Management for Hybrid Electric Vehicles. *IEEE Transactions on Vehicular Technology* **2008**, *57*, 3428–3440.

[21] Liu, T.; Zou, Y.; Liu, D.x.; Sun, F.c. Real-time control for a parallel hybrid electric vehicle based on Pontryagin's Minimum Principle. 2014 IEEE Conference and Expo Transportation Electrification Asia-Pacific (ITEC Asia-Pacific). IEEE, 2014, pp. 1–5.

[22] Ouddah, O.; Adouane, L.; Abdrakhmanov, R. From Offline to Adaptive Online Energy Management Strategy of Hybrid Vehicle Using Pontryagin's Minimum Principle. *Int. J. Automot. Technol. Vol.* **2017**, *19*, 571–584.

[23] Sivertsson, M. Adaptive Control Using Map-Based ECMS for a PHEV. *IFAC Proceedings Volumes* **2012**, *45*, 357–362.

[24] Zhang, F.; Xu, K.; Li, L.; Langari, R. Comparative Study of Equivalent Factor Adjustment Algorithm for Equivalent Consumption Minimization Strategy for HEVs. 2018 IEEE Vehicle Power and Propulsion Conference (VPPC). IEEE, 2018, pp. 1–7.

[25] Fu, Z.; Liu, X. Equivalent Consumption Minimization Strategy Based on a Variable Equivalent Factor. IEEE 2017 Chinese Automation Congress (CAC) 20-22 Oct. 2017 DOI: 10.1109/CAC.2017.8243519 . **2017**.

[26] Enang, W.; Bannister, C. Robust proportional ECMS control of a parallel hybrid electric vehicle. *Proceedings of the Institution of Mechanical Engineers, Part D: Journal of Automobile Engineering* **2017**, *231*, 99–119.

[27] Emre Kural, Bilin Aksun Güvenc. Predictive-Equivalent Consumption Minimization Strategy for Energy Management of A Parallel Hybrid Vehicle for Optimal Recuperation.

[28] Deufel, F.; Gießler, M.; Gauterin, F. A Generic Prediction Approach for Optimal Control of Electrified Vehicles Using Artificial Intelligence. *Vehicles* **2022**, *4*, 182–198.

[29] Deufel, F.; Gießler, M.; Gauterin, F. Optimal Control of Electrified Powertrains in Offline and Online Application Concerning Dimensioning of Li-Ion Batteries. *Vehicles* **2022**, *4*, 464–481.

[30] Deufel, F.; Jhaveri, P.; Harter, M.; Gießler, M.; Gauterin, F. Velocity Prediction Based on Map Data for Optimal Control of Electrified Vehicles Using Recurrent Neural Networks (LSTM). *Vehicles* **2022**, *4*, 808–824.

[31] Gao, A.; Deng, X.; Zhang, M.; Fu, Z. Design and Validation of Real-Time Optimal Control with ECMS to Minimize Energy Consumption for Parallel Hybrid Electric Vehicles. *Mathematical Problems in Engineering* **2017**, *2017*, 1–13.

[32] Görke, D. *Untersuchungen zur Kraftstoffoptimalen Betriebsweise von Parallelhybridfahrzeugen und darauf basierende Auslegung regelbasierter Betriebsstrategien*; Springer: Wiesbaden, Germany, 2016. https://doi.org/10.1007/978-3-658-14163-9.

[33] Bouwman, K.R.; Pham, T.H.; Wilkins, S.; Hofman, T. Predictive Energy Management Strategy Including Traffic Flow Data for Hybrid Electric Vehicles. *IFAC-PapersOnLine* **2017**, *50*, 10046–10051.

[34] Di Chen.; Kim, Y.; Stefanopoulou, A.G. Predictive Equivalent Consumption Minimization Strategy With Segmented Traffic Information. *IEEE Transactions on Vehicular Technology* **2020**, *69*, 14377–14390.

[35] Emre Kural, Bilin Aksun Güvenc. Predictive-Equivalent Consumption Minimization Strategy for Energy Management of A Parallel Hybrid Vehicle for Optimal Recuperation.

[36] Han, J.; Kum, D.; Park, Y. Synthesis of Predictive Equivalent Consumption Minimization Strategy for Hybrid Electric Vehicles Based on Closed-Form Solution of Optimal Equivalence Factor. *IEEE Transactions on Vehicular Technology* **2017**, *66*, 5604–5616.

[37] Kazemi, H.; Fallah, Y.P.; Nix, A.; Wayne, S. Predictive AECMS by Utilization of Intelligent Transportation Systems for Hybrid Electric Vehicle Powertrain Control. *IEEE Transactions on Intelligent Vehicles* **2017**, *2*, 75–84.

[38] Zhang, F.; Xi, J.; Langari, R. Real-Time Energy Management Strategy Based on Velocity Forecasts Using V2V and V2I Communications. *IEEE Transactions on Intelligent Transportation Systems* **2017**, *18*, 416–430.

Presenter Biography

Felix Deufel received the M. Sc. degree in Automotive Engineering in 2019 from the Technical University of Berlin, Berlin, Germany. He is currently working towards the Ph.D. degree on the energy management of hybrid electric vehicles (HEV) at KIT Institute of Vehicle Systems Technology Karlsruhe, Germany, in cooperation with Mercedes-Benz AG, Sindelfingen, Germany. His research interests lie in the fields of control and the application of Machine Learning.

Malte Freund received the B. Sc. degree in Electrical and Information Technology in 2022 from Karlsruhe Institute of Technology (KIT), Karlsruhe, Germany. He is currently studying towards the M.Sc. degree. His research interests lie in the fields of control and optimization of dynamic systems.

Frank Gauterin received the Diploma in physics from the University of Münster, Münster, Germany, in 1989 and the Dr. rer. nat. degree (Ph.D.) in physics from the University of Oldenburg, Oldenburg, Germany, in 1994. From 1989 to 2006, he was in different R&D positions with Continental AG, Germany, leaving as the Director of NVH Engineering (noise, vibration, harshness). Since 2006, he has been a Full Professor of the Karlsruhe Institute of Technology (KIT), Karlsruhe, Germany. He is the Head with the KIT Institute of Vehicle System Technology and scientific spokesperson of the KIT Center Mobility Systems. His research interests include vehicle control, vehicle dynamics, vehicle NVH, vehicle suspension, tire dynamics, and tire-road interaction as well as vehicle concepts, vehicle modeling, and identification methods.